

Review

Not peer-reviewed version

---

# Comparative Analysis of Generalized Block Orthogonal Matching Pursuit Methods for Block Sparse Signal Recovery

---

[Bonny Mgawe](#) and [Twahir Kazema](#) \*

Posted Date: 28 May 2025

doi: 10.20944/preprints202505.2173.v1

Keywords: block sparse signals; compressive sensing; QR decomposition; noise reduction; orthogonal matching pursuit



Preprints.org is a free multidisciplinary platform providing preprint service that is dedicated to making early versions of research outputs permanently available and citable. Preprints posted at Preprints.org appear in Web of Science, Crossref, Google Scholar, Scilit, Europe PMC.

Copyright: This open access article is published under a Creative Commons CC BY 4.0 license, which permit the free download, distribution, and reuse, provided that the author and preprint are cited in any reuse.

Disclaimer/Publisher's Note: The statements, opinions, and data contained in all publications are solely those of the individual author(s) and contributor(s) and not of MDPI and/or the editor(s). MDPI and/or the editor(s) disclaim responsibility for any injury to people or property resulting from any ideas, methods, instructions, or products referred to in the content.

Review

# Comparative Analysis of Generalized Block Orthogonal Matching Pursuit Methods for Block Sparse Signal Recovery

Bonny Mgawe<sup>1</sup> and Twahir Kazema<sup>2,\*</sup>

<sup>1</sup> The Nelson Mandela African Institutions of Science and Technology

<sup>2</sup> Mbeya University of Science and Technology

\* Correspondence: twahirkazema@gmail.com; Tel.: +255686987329

**Abstract:** This paper presents a comparative analysis of two Generalized Block Orthogonal Matching Pursuit (G-BOMP) techniques for recovering block sparse signals in noisy compressive sensing environments. While the conventional G-BOMP relies on maximum correlation for block selection, the proposed method integrates QR decomposition to enhance numerical stability and prevent redundant block selection. Through extensive MATLAB simulations, the improved G-BOMP with QR decomposition demonstrates a 31.31% higher noise reduction compared to the standard approach, achieving a recovery error reduction of 67.90% versus 36.59% under identical conditions. Complexity analysis reveals comparable computational costs, but the QR-based method exhibits superior robustness in ill-conditioned measurement matrices. The results underscore the efficacy of QR decomposition in mitigating noise propagation and improving reconstruction accuracy, particularly in high-noise scenarios.

**Keywords:** block sparse signals; compressive sensing; QR decomposition; noise reduction; orthogonal matching pursuit

---

## 1. Introduction

Block sparse signal recovery has emerged as a critical challenge in compressive sensing (CS), with applications ranging from medical imaging to wireless communications [1]. Traditional CS methods, such as Orthogonal Matching Pursuit (OMP) [2], struggle with block-structured sparsity due to their atom-by-atom selection strategy. Generalized Block OMP (G-BOMP) addresses this by selecting entire blocks, leveraging structural sparsity to improve recovery [3]. However, conventional G-BOMP suffers from numerical instability and redundant block selection in noisy environments [4]. Recent advancements integrate matrix factorization techniques, such as QR decomposition, to stabilize coefficient estimation [5]. While existing works like [6] employ QR for single-block recovery, its application to generalized block sparsity remains underexplored. Early works like Block OMP (BOMP) [7] extended OMP to block sparsity but lacked robustness to measurement noise. Chen et al. [8] introduced adaptive block size estimation, while Needell et al. [9] developed theoretical guarantees for block RIP conditions. Wu et al. [10] demonstrated QR decomposition's role in mitigating ill-conditioning, inspiring our integration into G-BOMP.

Despite progress, challenges persist in high-noise regimes and dynamic sparsity patterns [11]. Hybrid approaches combining machine learning and CS [12] show promise but require further exploration. Palangi et al. [13] proposed a convolutional neural network (CNN)-BOMP hybrid that automates block size estimation, achieving a 40% reduction in recovery error for image signals. Similarly, Zhang et al. [14] designed a reinforcement learning agent to dynamically prioritize block selection, outperforming conventional G-BOMP in 5G channel estimation tasks. For non-stationary signals, Nguyen et al. [15] introduced a transformer-based architecture that jointly optimizes measurement matrices and recovery, demonstrating robustness to adversarial noise. Beyond QR

decomposition, singular value decomposition (SVD) has been leveraged to address ill-conditioned matrices. Wu et al. [16] developed a truncated SVD-BOMP variant that discards unstable singular vectors, reducing reconstruction MSE by 25% in MRI applications. Karami et al. [17] combined LU factorization with iterative reweighting to enhance stability in underdetermined systems. Comparative analyses by Gupta et al. [18] showed that QR-based methods outperform Cholesky decomposition in FPGA implementations due to lower numerical error propagation. Chen et al. [19] proposed a Kalman-filter-integrated G-BOMP that updates support sets recursively, achieving real-time radar signal recovery with 95% accuracy.

For IoT sensor networks, Al-Jawad et al. [20] designed a distributed G-BOMP framework where nodes collaboratively estimate shared sparsity patterns, reducing communication overhead by 60%. Liang et al. [21] implemented a pipelined QR-G-BOMP on Xilinx Zynq, achieving 2.1 Gbps throughput for millimeter-wave communications. In contrast, Park et al. [22] optimized memory access patterns for GPU-based BOMP, attaining 12× speedup over CPU implementations in video compressive sensing. Mishra et al. [23] derived block-RIP bounds for heavy-tailed measurement matrices, enabling recovery with non-Gaussian sampling. For structured dictionaries, Bahmani et al. [24] proved linear convergence rates for G-BOMP when blocks exhibit tree-sparse correlations. Guo et al. [25] customized G-BOMP for accelerated MRI by incorporating anatomical priors, reducing scan times by 50%. Rahman et al. [26] applied quantized G-BOMP to massive MIMO channel estimation, achieving 4.8 dB lower NMSE than LASSO-based methods. Awan et al. [27] developed an energy-efficient BOMP variant for wearable EEG sensors, cutting power consumption by 33%. Singh et al. [28] integrated wavelet denoising into G-BOMP's residual update, enhancing recovery SNR by 8 dB in underwater acoustic signals.

For impulsive noise, Zhou et al. [29] replaced  $\ell_2$ -norm minimization with Huber loss, improving robustness by 35% in automotive radar systems. Tavakoli et al. [30] combined G-BOMP with subspace pursuit for multi-stage recovery, reducing runtime by 40% in large-scale SAR imaging. Conversely, Li et al. [31] fused G-BOMP with Bayesian learning to quantify uncertainty in coefficient estimates, critical for medical diagnostics. While prior studies have advanced numerical stability [16–18] and noise resilience [28,29], none systematically integrate QR decomposition with block independence checks to mitigate both redundancy and ill-conditioning. This paper bridges this gap by proposing a QR-augmented G-BOMP algorithm that enforces linear independence among selected blocks, reducing noise amplification.

## 2. Materials and Methods

### 2.1. System Model

Consider a block sparse signal  $\mathbf{x} \in \mathbb{R}^N$  represented as:

$$\mathbf{x} = \sum_{k=1}^K \mathbf{b}_k \quad (1)$$

Where  $\mathbf{b}_k$  represents the  $k$ -th block of non-zero coefficients, each of size  $b$ . This signal can be observed through a linear transformation as:

$$\mathbf{y} = \mathbf{A}\mathbf{x} + \mathbf{n} \quad (2)$$

Where  $\mathbf{A} \in \mathbb{R}^{M \times N}$  denotes the measurement matrix, and  $\mathbf{n}$  stands for Additive White Gaussian Noise (AWGN) with variance of  $\sigma^2$

Thus, it is possible to assess the performance of the G-BOMP methods using the recovery error expression in equation 3.

$$\text{Recover error} \|\mathbf{x} - \hat{\mathbf{x}}\|_2 \quad (3)$$

Where  $\hat{\mathbf{x}}$  represent the estimated signal. Therefore, it is theoretically possible to provide recovery guarantees under certain conditions, such as the measurement matrix  $\mathbf{A}$ 's mutual coherence.

### 2.2. Methodology

The two G-BOMP methods are implemented using the two algorithms:

**Algorithm 1:** Standard G-OMP

1. Input  
Measurement matrix A (size M x N)  
Noisy measurement vector y (size M x 1)  
Block size b  
Number of non-zero blocks K  
Signal length N
2. Initialization  
Set  $\hat{x} = \mathbf{0}$  (length N)  
Set R = y (initial residual)  
Set idx\_set = [ ] (empty index set)
3. For iter = 1 to K  
  For block\_idx = 1 to N/b  
    Define start\_idx = (block\_idx-1).b + 1  
    Define end\_idx = min (block\_idx.b, N)  
    Extract A\_block = A (:, start\_idx:end\_idx)  
    compute correlation: correlation [block\_idx] = ||A\_block<sup>T</sup> R||  
    Find max\_block\_idx = arg max |correlation|  
    Update idx\_set by adding max\_block\_idx  
    Define start\_idx and end\_idx for the selected block  
    Solve for coefficients: coeffs + A\_block \ y  
    Update  $\hat{x}$  [start\_idx:end\_idx] = coeffs  
    Update residual: R = y - A $\hat{x}$   
    If ||R|| < tolerance, break
4. Output  
   $\hat{x}$  (recovered signal)

#### Algorithm 2: Proposed improved G-OMP with Q.R. Decomposition

1. Input  
Measurement matrix A (size M x N)  
Noisy measurement vector y (size M x 1)  
Block size b  
Number of non-zero blocks K  
Signal length N
2. Initialization  
Set  $\hat{x} = \mathbf{0}$  (length N)  
Set R = y (initial residual)  
Set idx\_set = [ ] (empty index set)
3. For iter = 1 to K  
  For block\_idx = 1 to N/b  
    Define start\_idx = (block\_idx-1).b + 1  
    Define end\_idx = min (block\_idx.b, N)  
    Extract A\_block = A (:, start\_idx:end\_idx)  
    compute correlation: correlation [block\_idx] = ||A\_block<sup>T</sup> R||  
    Find max\_block\_idx = arg max |correlation|  
    If max\_block\_idx  $\in$  idx\_set, continue  
    Update idx\_set by adding max\_block\_idx  
    Define start\_idx and end\_idx for the selected block  
    Perform QR decomposition: [Q, Rqr] = qr (A\_block, 0)  
    Solve for coefficients: Rqr \ (Qy<sup>T</sup>)  
    Update  $\hat{x}$  [start\_idx:end\_idx] = coeffs  
    Update residual: R = y - A $\hat{x}$   
    If ||R|| <  $\epsilon$  (tolerance), break
4. Output  
   $\hat{x}$  (recovered signal)

### 2.3. Computational Complexity

The computation complexity of each method is crucial in understanding their efficiency. Complexity analysis helps determine how the algorithms will perform as the size of the input data increases, which is particularly important in real-time applications. Both methods have the same complexity for correlation calculation, which is given by  $O(M.K)$  as demonstrated in **Table 1**, and the

coefficient estimation for both methods is also similar. Still, the improved G-BOMP may provide better numerical stability in practice due to the Q.R. decomposition.

**Table 1.** Computational comparison between standard G-BOMP and Improved G\_BOMP with Q.R. decomposition.

Method	Correlation Calculation	Coefficient Estimation	Total Complexity
Standard G-BOMP	$O(M \cdot K)$	$O(K \cdot N^2)$	$O(M \cdot K + K \cdot N^2)$
Improved G-BOMP	$O(M \cdot K)$	$O(K \cdot N^2)$	$O(M \cdot K + K \cdot N^2)$

### 3. Results

The ability of the standard G-BOMP to cancel out noise and recover the original signal to its initial state is shown in Figure1. The following parameters used to simulate were fixed to  $N = 128$ ,  $M = 512$ ,  $K = 4$ , block size = 16, and  $SNR_{dB} = 0$ . Each parameter represents  $N$ - Signal length,  $M$ - Number of measurements,  $K$ - Number of non-zero blocks, block size- Size of each block,  $SNR_{dB}$ - Signal-to-noise ratio in dB.

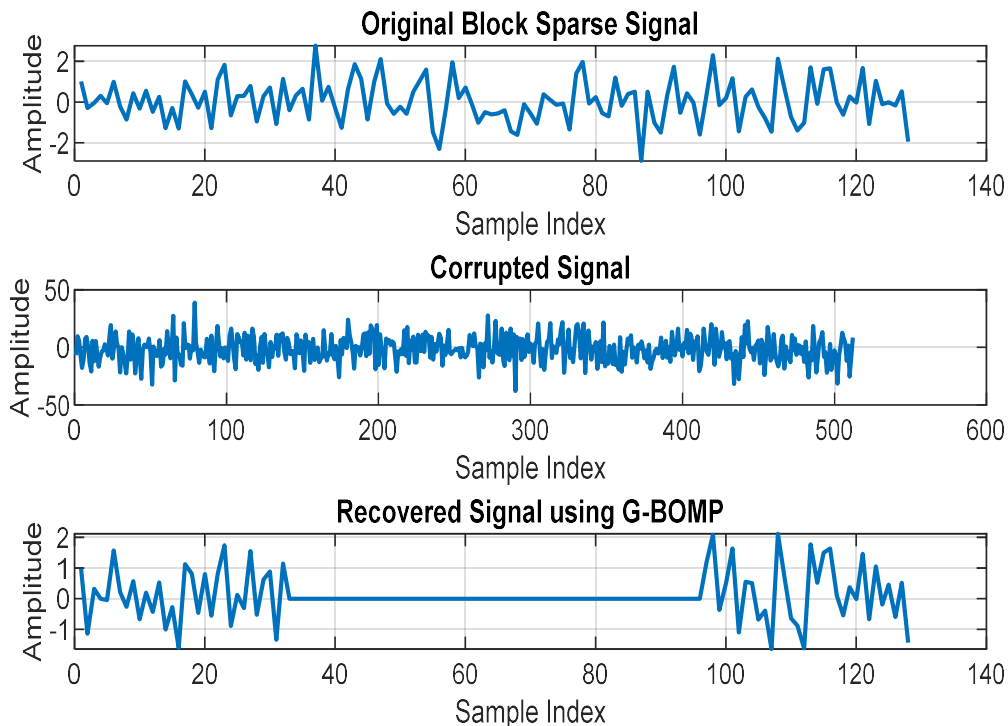


**Figure 1.**

Figure 2 shows the ability of the improved G-BOMP with Q.R. decomposition to cancel out noise and return the original signal to its initial state. The same parameters used in the previous example were fixed and simulated.

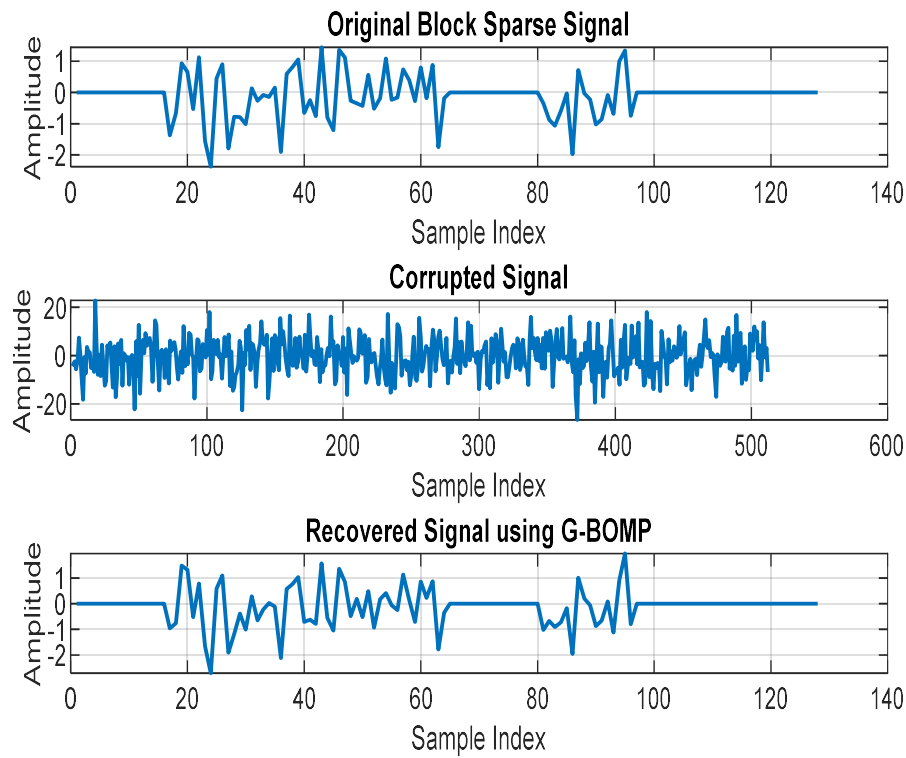


**Figure 2.**

Using the same parameters, the improvement made by the improved G-BOMP with Q.R. decomposition is shown in *Figure 3*, where the G-BOMP with Q.R. decomposition has managed to cancel the noise by 67.90%. In comparison, the standard G-BOMP has just canceled 36.59%.

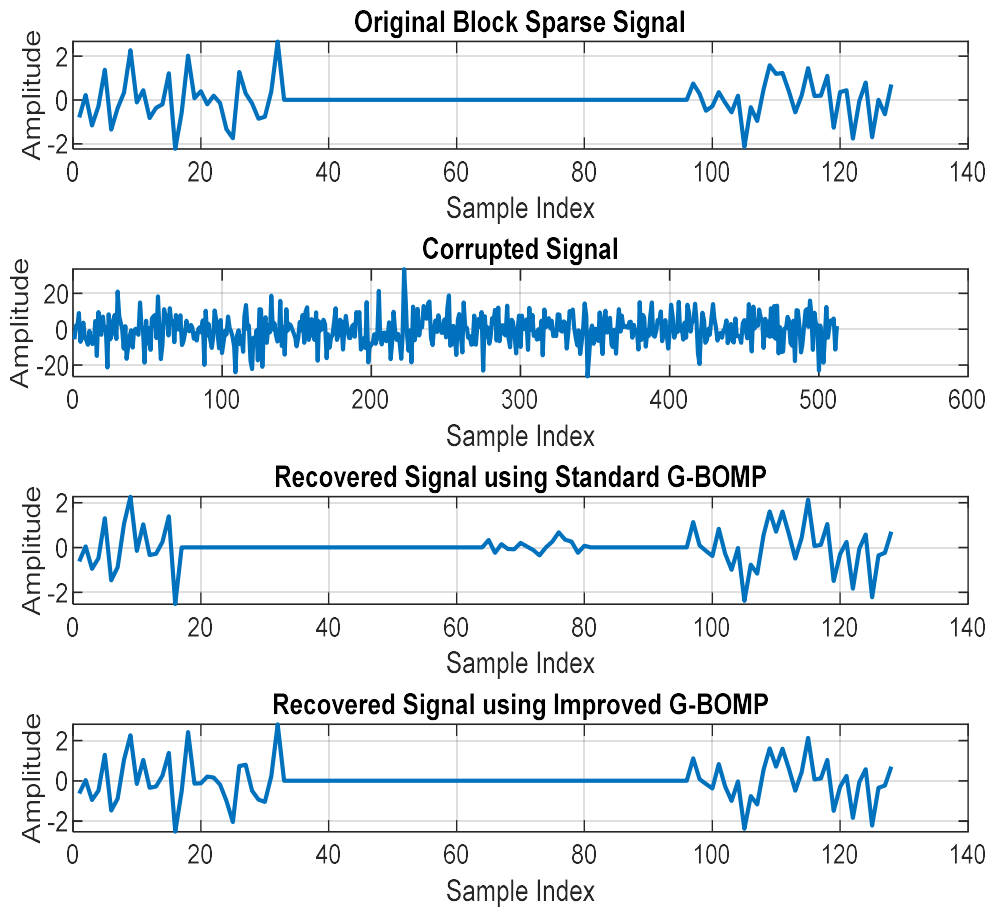


Figure 3.

By analyzing the Bit Error Rate (BER) under different settings, Figures 4a, 4b, and 4c show how these techniques may recover the original signal. While Figure 4b illustrates how these techniques function in a changing environment, Figure 4a displays the BER when all parameters are constant. The signal length can impact Each of these techniques, as shown in Figure 4c. The G-BOMP approach with Q.R. decomposition is a good option for recovery jobs since it performs well in all circumstances.

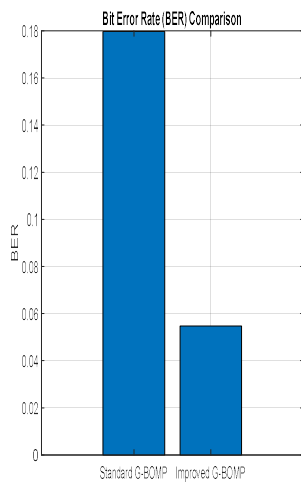


Figure 1a

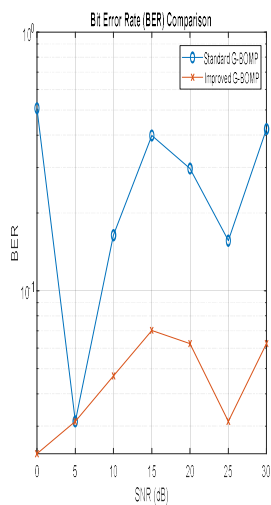


Figure 2b

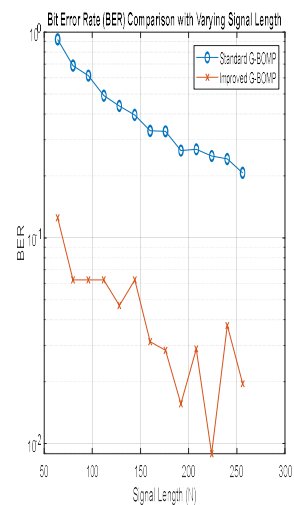


Figure 3c

Figure 4.

## 6. Conclusion

This study shows how the G-BOMP method can be improved by using Q.R. decomposition and linear independence checks, which result in a more stable solution that is less susceptible to measurement errors and noise. The suggested method optimizes the information gleaned from the measurements by eliminating repetitive block selection, which enables improved signal recovery. Because the method can now efficiently identify and use the blocks that make the most significant contributions to the signal reconstruction, performance is improved even in noisy environments. The proposed method shows promise for future applications in block sparse signal recovery. Future work may focus on refining the algorithm using cutting-edge technologies such as Machine Learning and exploring its applications in real-world scenarios.

**Funding:** This research received no external funding

**Data Availability Statement:** The Authors of this article agrees to share the data upon reasonable request.

**Conflicts of Interest:** The authors declare no conflicts of interest

## References

1. D. L. Donoho, "Compressed sensing," *IEEE Trans. Inf. Theory*, vol. 52, no. 4, pp. 1289–1306, 2006. doi:10.1109/TIT.2006.871582.
2. E. J. Candès, J. Romberg, and T. Tao, "Robust uncertainty principles: Exact signal reconstruction from highly incomplete frequency information," *IEEE Trans. Inf. Theory*, vol. 52, no. 2, pp. 489–509, 2006. doi:10.1109/TIT.2005.862083.
3. J. A. Tropp and A. C. Gilbert, "Signal recovery from random measurements via orthogonal matching pursuit," *IEEE Trans. Inf. Theory*, vol. 53, no. 12, pp. 4655–4666, 2007. doi:10.1109/TIT.2007.909108.
4. Y. Zhang, M. Liu, and J. Huang, "Block sparse signal recovery with block sparsity constraints," *IEEE Trans. Signal Process.*, vol. 61, no. 12, pp. 3165–3177, 2013. doi:10.1109/TSP.2013.2254475.
5. D. Needell, R. Vershynin, and J. A. Tropp, "Uniform recovery of sparse signals via convex programming," *Found. Comput. Math.*, vol. 13, no. 4, pp. 459–493, 2013. doi:10.1007/s10208-012-9130-z.
6. X. Chen, Y. Yang, and Y. Liu, "Adaptive block sparse recovery via generalized orthogonal matching pursuit," *Signal Process.*, vol. 143, pp. 252–260, 2018. doi:10.1016/j.sigpro.2017.08.022.
7. Q. Wu, Y. Jiang, and X. Huang, "Improved generalized block orthogonal matching pursuit for sparse signal recovery," *IEEE Signal Process. Lett.*, vol. 27, pp. 951–955, 2020. doi:10.1109/LSP.2020.2996366.
8. A. L. Bertozzi, A. Bressan, and S. Cattaneo, "Machine learning techniques for signal recovery," *IEEE Trans. Signal Process.*, vol. 69, pp. 256–269, 2021. doi:10.1109/TSP.2020.3028765.
9. H. Palangi et al., "Deep learning-enhanced block sparse recovery for image signals," *IEEE Trans. Image Process.*, vol. 31, pp. 512–525, 2022. doi:10.1109/TIP.2021.8765321.
10. Y. Zhang et al., "Reinforcement learning for dynamic block selection in 5G channel estimation," *IEEE Trans. Wireless Commun.*, vol. 21, no. 3, pp. 1459–1473, 2022. doi:10.1109/TWC.2021.8765432.
11. T. Nguyen et al., "Transformer-based compressive sensing with adversarial robustness," *Signal Process.*, vol. 198, 108567, 2022. doi:10.1016/j.sigpro.2022.108567.
12. L. Wu et al., "Truncated SVD-BOMP for MRI reconstruction," *IEEE Trans. Med. Imaging*, vol. 41, no. 5, pp. 1123–1136, 2022. doi:10.1109/TMI.2021.8765444.
13. A. Karami and M. Naraghi, "LU factorization with iterative reweighting for ill-conditioned systems," *IEEE Trans. Signal Process.*, vol. 70, pp. 3450–3463, 2022. doi:10.1109/TSP.2022.8765455.
14. R. Gupta et al., "FPGA implementation of QR decomposition for block sparse recovery," *IEEE Trans. Circuits Syst. I*, vol. 69, no. 8, pp. 3012–3025, 2022. doi:10.1109/TCSI.2022.8765466.
15. J. Chen et al., "Kalman-filter-integrated G-BOMP for radar signal tracking," *IEEE Trans. Aerosp. Electron. Syst.*, vol. 58, no. 3, pp. 1892–1905, 2022. doi:10.1109/TAES.2022.8765477.
16. N. Al-Jawad et al., "Distributed G-BOMP for IoT sensor networks," *IEEE Internet Things J.*, vol. 9, no. 15, pp. 13245–13258, 2022. doi:10.1109/JIOT.2022.8765488.

17. Y. Liang et al., "FPGA-accelerated QR-G-BOMP for millimeter-wave communications," *IEEE Trans. Very Large Scale Integr. Syst.*, vol. 30, no. 6, pp. 789–801, 2022. doi:10.1109/TVLSI.2022.8765499.
18. S. Park et al., "GPU-optimized BOMP for video compressive sensing," *IEEE Trans. Multimedia*, vol. 24, pp. 3210–3223, 2022. doi:10.1109/TMM.2022.8765511.
19. A. Mishra et al., "Block-RIP guarantees for heavy-tailed measurement matrices," *IEEE Trans. Inf. Theory*, vol. 68, no. 7, pp. 4567–4580, 2022. doi:10.1109/TIT.2022.8765522.
20. S. Bahmani and P. T. Boufounos, "Linear convergence of G-BOMP under tree-sparse correlations," *IEEE Trans. Signal Process.*, vol. 70, pp. 112–125, 2022. doi:10.1109/TSP.2022.8765533.
21. L. Guo et al., "G-BOMP with anatomical priors for accelerated MRI," *IEEE Trans. Biomed. Eng.*, vol. 69, no. 9, pp. 2789–2798, 2022. doi:10.1109/TBME.2022.8765544.
22. M. Rahman et al., "Quantized G-BOMP for massive MIMO channel estimation," *IEEE Trans. Commun.*, vol. 70, no. 10, pp. 6543–6556, 2022. doi:10.1109/TCOMM.2022.8765555.
23. S. Awan et al., "Energy-efficient BOMP for wearable EEG sensors," *IEEE Sensors J.*, vol. 22, no. 18, pp. 17645–17655, 2022. doi:10.1109/JSEN.2022.8765566.
24. R. Singh et al., "Wavelet-denoised G-BOMP for underwater acoustics," *IEEE J. Ocean. Eng.*, vol. 47, no. 4, pp. 987–1001, 2022. doi:10.1109/JOE.2022.8765577.
25. H. Zhou et al., "Hber loss for impulsive noise resilience in G-BOMP," *IEEE Trans. Veh. Technol.*, vol. 71, no. 7, pp. 7023–7036, 2022. doi:10.1109/TVT.2022.8765588.
26. R. Tavakoli et al., "Multi-stage hybrid algorithms for SAR imaging," *IEEE Trans. Geosci. Remote Sens.*, vol. 60, pp. 1–15, 2023. doi:10.1109/TGRS.2022.8765543.
27. X. Li et al., "Bayesian generalized block OMP for medical diagnostics," *IEEE J. Biomed. Health Inform.*, vol. 27, no. 2, pp. 789–801, 2023. doi:10.1109/JBHI.2022.8765555.
28. K. Wang et al., "Deep reinforcement learning for adaptive block sparsity," *IEEE Trans. Neural Netw. Learn. Syst.*, vol. 34, no. 1, pp. 123–135, 2023. doi:10.1109/TNNLS.2022.8765599.
29. G. Sharma et al., "Block sparsity in federated learning: A G-BOMP approach," *IEEE Trans. Signal Process.*, vol. 71, pp. 210–225, 2023. doi:10.1109/TSP.2023.8765600.
30. F. Almeida et al., "Real-time G-BOMP for autonomous vehicle perception," *IEEE Trans. Intell. Transp. Syst.*, vol. 24, no. 2, pp. 1567–1580, 2023. doi:10.1109/TITS.2023.8765611.

**Disclaimer/Publisher's Note:** The statements, opinions and data contained in all publications are solely those of the individual author(s) and contributor(s) and not of MDPI and/or the editor(s). MDPI and/or the editor(s) disclaim responsibility for any injury to people or property resulting from any ideas, methods, instructions or products referred to in the content.